Production of heavy spin-$\frac{3}{2}$ fermions in colliders

B. Moussallam and V. Soni
Division de Physique Théorique, Institut de Physique Nucléaire, Université Paris–Sud, 91406 Orsay, France
(Received 16 August 1988)

If very heavy quarks exist in the standard model, it is likely that spin-$\frac{3}{2}$ excited states will arise. Moreover, a recent model indicates that deeply bound nucleonlike bound states having a nearby spin-$\frac{3}{2}$ excitation will be present. We calculate production rates for creating pairs of color-singlet or -triplet spin-$\frac{3}{2}$ fermions in proton-(anti)proton colliders. In pointlike approximation, the rates turn out to be considerably larger than those for ordinary fermions. We estimate the influence of form factors, making some reasonable guesses. We show that very different decay patterns emerge depending whether or not these states are pointlike. We estimate that the Superconducting Super Collider could uncover spin-$\frac{3}{2}$ quarks up to a mass around 1 TeV.

I. INTRODUCTION

Colliders with a $\sqrt{s}$ of a few tens of TeV, such as the Superconducting Super Collider (SSC) or the CERN Large Hadron Collider (LHC), are being planned for the next decade. It is tempting to start from now to attempt to figure out what particles may be discovered with this kind of machine. At present, most of the ingredients of the standard electroweak model have been found, with two notable exceptions: the top quark (the latest lower bound on its mass is $\simeq 45$ GeV (Ref. 1) and the Higgs boson. Beyond the standard model the simplest guess is to imagine that there are new generations of quarks and leptons. A large number of production reaction rates for SSC-like colliders, involving known as well as unknown particles, have been calculated in the vast review of Eichten, Hinchliffe, Lane, and Quigg.[2] More recently, new mechanisms were suggested for the production of heavy-lepton pairs.[3,4] Concerning quarks, while the basics were initiated some time ago,[5] calculations to order α_s^3 have been completed very recently,[6] stimulated by the availability of experimental results on charm and bottom production. A survey of production and decay signatures of heavy quarkonium can be found in Ref. 7. In this work, we discuss the production of spin-$\frac{3}{2}$ fermions.

One motivation may be that if such objects are colored and coexist with ordinary quarks in a range between, say, 0.5 and 1 TeV, they may be much easier to produce. This is one outcome of our calculations but it may have been expected, to some extent, from the start. As for quarks, the main production mechanism is provided by gluon-gluon fusion. It is known that the cross section for two gluons $\rightarrow$ two gluons is significantly larger than two gluons $\rightarrow q\bar{q}$, mainly because it involves a spin-one particle exchange in the cross channel, instead of a spin $\frac{1}{2}$. An even larger enhancement caused by spin-$\frac{3}{2}$ exchange will be seen to arise here.

There are some theoretical motivations as well. For instance, Johnson and Schechter[8] have developed a semiclassical picture of mass generation for heavy fermions in the standard model, based on an analogy with the linear σ model. Some aspects of this picture are further elaborated in Ref. 9. The relevance of the σ model is made clear if one writes down the Higgs-field doublet in the following way:

$$\sqrt{2}\Phi = \begin{bmatrix} \pi_2 + i\pi_1 \\ \sigma - i\pi_0 \end{bmatrix} . \tag{1}$$

When the Yukawa coupling gets large enough, it is argued that classical solutions of the equations of motion where σ and π acquire a so-called Skyrme-hedgehog (solitonic) configuration[10] become relevant, rather than the usual one $\sigma = v$, $\pi = 0$. Let us only recall here the main two conclusions of this approach. Assuming the presence of a heavy enough quark doublet (to be called U and D in the following), (a) there arises an excited multiplet with spin $\frac{3}{2}$ and also isospin $\frac{3}{2}$ and (b) the heavy quarks can form deeply bound color singlets analogous to nucleons, which also possess spin-$\frac{3}{2}$ excitations. Typical results for the masses are

$$m_Q \simeq 2\,\text{TeV}, \quad m_{Q^*} \simeq 4\,\text{TeV} ,$$

$$m_N \simeq 2\,\text{TeV}, \quad m_{N^*} \simeq 2.5\,\text{TeV} .$$

Unfortunately, it is practically out of the question to provide reliable estimates for the production of fermions above 1 TeV, as the interaction in the final state becomes nonperturbative. (In the spin-$\frac{1}{2}$ case unitarity violations occur even below that.[11]) We shall make predictions for masses below 1 TeV only. In fact, above this energy, perturbative calculations probably provide rather wide upper bounds, which tend to indicate that the cross sections for producting 2-TeV fermions would be much too small to be observed anyway. These results on the masses may, after all, be only indicative while the main ideas may apply to fermions with masses of a few hundred GeV only. Indeed, the same authors have shown subsequently that varying the Higgs-boson self-coupling may result in lowering the masses significantly.[12] For those who do not like this model, we note that on the basis of the Chew-Low mechanism[13] one would also predict that spin-$\frac{3}{2}$

quarks occur with moderately larger masses than the spin-$\frac{1}{2}$ ones, provided the Yukawa coupling constant is strong enough.

A distinctive aspect of this kind of picture is the expectation of rather large form factor effects. We found it difficult to treat these better than qualitatively; this is done in Sec. IV. One may alternatively imagine that pointlike spin-$\frac{3}{2}$ quarks exist, a picture which could be valid if the mass is as low as, say, 100 GeV. We investigate this possibility, assuming further that the multiplet has a weak-isospin-$\frac{3}{2}$ assignment. Some features of the decay properties of excited quarks are then discussed in Sec. V, which turn out to be rather different from those predicted in Refs. 8 and 9. In Sec. III one can find the main results of our cross-section calculations, while in Sec. II we have collected all the interaction Lagrangians needed to perform them.

II. LAGRANGIANS AND COUPLINGS

The Lagrangian for a free spin-$\frac{3}{2}$ particle was established a long time ago.[14] To look more modern, let us use the form suggested in the supergravity literature:[15]

$$\mathcal{L}_0=-\varepsilon^{\mu\nu\rho\sigma}\bar{\psi}_\mu\gamma_5\gamma_\nu\partial_\rho\psi_\sigma+im\bar{\psi}_\mu\sigma^{\mu\nu}\psi_\nu\ . \tag{2}$$

ψ_μ is the Rarita-Schwinger spinor which [as a consequence of (2)] satisfies $\partial^\mu\psi_\mu=\gamma^\mu\psi_\mu=0$. The following propagator corresponds to $\mathcal{L}_0$:

$$\begin{aligned}\mathcal{P}^{\mu\nu}&=-\frac{1}{p^2-m^2}\Lambda^{\mu\nu}\ ,\\ \Lambda^{\mu\nu}&=\left[g^{\mu\nu}-\frac{p^\mu p^\nu}{m^2}\right](\not{p}+m)\\ &\quad+\frac{1}{3}\left[\gamma^\mu+\frac{p^\mu}{m}\right](\not{p}-m)\left[\gamma^\nu+\frac{p^\nu}{m}\right]\ .\end{aligned} \tag{3}$$

This choice corresponds to a unitary gauge in a supergravity context, which seems natural to adopt here (other opinions were expressed in the spin-$\frac{3}{2}$ literature[16]). To conclude with the free-particle description, we recall that ψ_μ can be redefined according to a one-parameter family of transformations:

$$\psi'_\mu=\psi_\mu+r\gamma_\mu\gamma\cdot\psi\ . \tag{4}$$

Our cross sections will not depend on these redefinitions.

The most interesting results will concern excited quarks. Let us assume that ψ_μ belongs to a color triplet; minimal coupling to QCD leaves us with the following:

$$\mathcal{L}_1=g_s\bar{\psi}_\mu(\gamma^\mu\gamma^\rho\gamma^\sigma-g^{\mu\rho}\gamma^\sigma-g^{\sigma\rho}\gamma^\mu+g^{\sigma\mu}\gamma^\rho)\frac{\lambda^a}{2}\psi_\sigma G^a_\rho\ . \tag{5}$$

Now if Q^* is an excited state corresponding to a heavy quark Q, it is likely that gluons will induce transitions between them. This kind of coupling will allow us to create pairs like $Q^*\bar{Q}$, which have a more favorable phase space than $Q^*\bar{Q}^*$. We point out that this coupling is not allowed in the solitonic model because its isospin symmetry would be violated. Furthermore, one has to assume that states of Q^* and Q with the same flavor exist. We envisage nevertheless this possibility, which is described by

$$\mathcal{L}_2=\frac{i\kappa g_s}{m+m_*}\bar{\psi}_\sigma(g^{\sigma\mu}-\tfrac{1}{4}\gamma^\sigma\gamma^\mu)\gamma^\nu\gamma^5\frac{\lambda^a}{2}\psi G^a_{\mu\nu}+\text{H.c.} \tag{6}$$

This is in analogy with the $\gamma N\Delta$ coupling, which was first considered a long time ago.[17] Note that the second term ensures here invariance under the transformation (4). The coupling being nonminimal, the parameter κ in (6) is left undetermined unless more detailed dynamical information is assumed. It is reasonable to expect it to be of order unity, and in the applications we shall fix its value to one. It is obviously possible to imagine more complicated couplings also, but we may assume that (6) will at least provide correct orders of magnitude.

Let us now turn to the electroweak couplings. We write down only those which are needed in either of the forthcoming sections, in particular, terms which vanish on shell are omitted. The neutral weak interaction, to begin with:

$$\mathcal{L}_3=\frac{e}{4\sin\theta_W\cos\theta_W}\bar{\psi}_\nu\gamma^\mu[2I_z(1-\gamma^5)-4Q\sin^2\theta_W]\psi^\nu Z_\mu\ . \tag{7}$$

According to our weak-isospin conventions, the eigenvalues of I_z will range from $-\frac{3}{2}$ to $\frac{3}{2}$ and the electric charge Q from $-\frac{4}{3}$ to $\frac{5}{3}$. In practice, electroweak interactions will give rise to negligible quark production cross sections (at least in the energy range under consideration here). On the contrary, they are of central importance for the production of colorless states, such as leptons or heavy bound states. In these cases, the charge in (7) takes on integer values and we may expect the presence of an axial-vector form factor g_a for the bound states.

Again here, we can imagine transition interactions between spin-$\frac{1}{2}$ and spin-$\frac{3}{2}$ states. Assuming that we want to keep SU(2)×U(1) gauge invariance, we have a larger freedom than in the case of QCD because now, we can have terms which contain gauge fields and Higgs fields at the same time. Let us delay the discussion of this possibility to Sec. V. The terms which do not involve Higgs fields must contain gauge-invariant tensors and also they must be proportional to an isospin transition matrix T. By analogy with (6) and the usual construction of the standard model, we arrive at

$$\begin{aligned}\mathcal{L}_4=\frac{\kappa e}{2s(m+m_*)}\bar{\psi}_\mu\gamma_\nu\gamma_5(1-\gamma_5)\Big[&T_+(\partial^\mu W^\nu_+-\partial^\nu W^\mu_+)+(+\to-)+T_z\frac{1}{c}(\partial^\mu Z^\nu-\partial^\mu Z^\mu)\\ &-i\frac{e}{s}[(T_+W^\mu_++T_-W^\mu_-)(cZ^\nu-sA^\nu)+W^\mu_+W^\nu_--(\mu\to\nu)]\Big]\psi+\text{H.c.}\ ,\end{aligned} \tag{8}$$

where s and c stand for $\sin\theta_W$ and $\cos\theta_W$, respectively, A is the photon field, and the isospin matrices are

$$T_- = -\begin{bmatrix} 0 & 0 \\ 0 & 0 \\ \frac{1}{\sqrt{3}} & 0 \\ 0 & 1 \end{bmatrix}, \quad T_+ = \begin{bmatrix} 1 & 0 \\ 0 & \frac{1}{\sqrt{3}} \\ 0 & 0 \\ 0 & 0 \end{bmatrix},$$

$$T_z = -\left[\frac{2}{3}\right]\begin{bmatrix} 0 & 0 \\ 0 & 1 \\ 1 & 0 \\ 0 & 0 \end{bmatrix}.$$

Finally, we shall need an estimate for the Higgs-boson couplings, which play a role in the production of colorless fermion pairs. We choose for the spin-$\frac{3}{2}$ case a form exactly analogous to the spin $\frac{1}{2}$:

$$\mathcal{L}_5 = g_y \bar{\psi}_\mu (g^{\mu\nu} - \gamma^\mu \gamma^\nu)\psi_\nu \Phi \ , \tag{9}$$

where the Yukawa coupling is taken to be $g_y = em_*/(\sqrt{2} m_W \sin\theta_W)$.

III. PRODUCTION CROSS SECTIONS IN POINTLIKE APPROXIMATION

The production rates in hadron-hadron collisions may be obtained through traditional parton-model ideas: one first computes an elementary scattering cross section between, say, two partons and then one integrates over the partonic distribution functions. For proton-proton collisions,

$$\sigma(p+p \to a+b+X) = \sum_{i,j} \int_{t_0}^1 dt \int_t^1 \frac{dx}{x} f_i(x) f_j(t/x) \hat{\sigma}_{i+j\to a+b}(ts) \ , \tag{10}$$

where i and j index the parton species, f_i is the corresponding distribution function (in the following, we use set 1 of Eichten *et al.*,[2] with $\Lambda = 200$ MeV). The lower integration bound, $t_0 = (m_a + m_b)^2/s$. The scale Q^2 which occurs in the structure functions and in α_s is taken to be the mass squared of the produced fermion.

A. $Q^* \bar{Q}^*$ pairs

The relevant graphs, to lowest order in α_s are represented in Fig. 1. Quark-antiquark fusion was included only for completeness, as its contribution may be expected to be negligible compared to gluon-gluon fusion. The amplitudes corresponding to the first three diagrams of Fig. 1 have the following expressions:

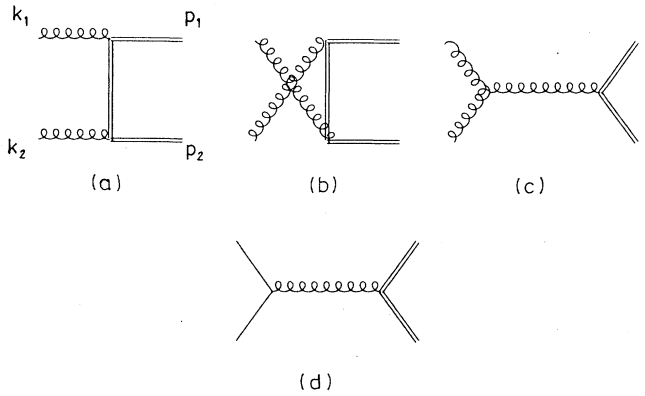

FIG. 1. Feynman graphs which contribute to the production of a spin-$\frac{3}{2}$ pair to order one in α_s. Double lines represent spin-$\frac{3}{2}$ fermions and single lines spin-$\frac{1}{2}$ ones.

$$\begin{aligned}
\mathcal{A}_t &= -g_s^2 \left[\frac{\lambda^b \lambda^c}{4}\right] \frac{1}{D_t} \bar{u}_\mu (-\varepsilon_1^\mu \gamma^\sigma + \not{\varepsilon}_1 g^{\mu\sigma}) \\
&\quad \times \Lambda_{\sigma\tau} (-\varepsilon_2^\nu \gamma^\tau + \not{\varepsilon}_2 g^{\nu\tau}) u_\nu \ , \\
\mathcal{A}_u &= -g_s^2 \left[\frac{\lambda^c \lambda^b}{4}\right] \frac{1}{D_u} \bar{u}_\mu (-\varepsilon_2^\mu \gamma^\sigma + \not{\varepsilon}_2 g^{\mu\sigma}) \\
&\quad \times \Lambda_{\sigma\tau} (-\varepsilon_1^\nu \gamma^\tau + \not{\varepsilon}_1 g^{\nu\tau}) u_\nu \ , \\
\mathcal{A}_s &= -g_s^2 \left[-i\frac{f^{abc}\lambda^a}{2}\right] \frac{1}{s} \bar{u}_\mu [\not{\varepsilon}_1 \varepsilon_2 \cdot (2k_1 + k_2) \\
&\qquad - \not{\varepsilon}_2 \varepsilon_1 \cdot (2k_2 + k_1) \\
&\qquad + \varepsilon_1 \cdot \varepsilon_2 (\not{k}_2 - \not{k}_1)] v^\mu \ ,
\end{aligned} \tag{11}$$

where the conventions for the momenta are shown in Fig. 1 and the spin-$\frac{3}{2}$ projector Λ is detailed in (3) (it has to be taken here with the proper momentum), $D_t = t - m^2, t, u\ s$ are the usual Mandelstam variables relevant to the partonic subprocess, and similarly with D_u.

Next, the trace computations can be performed using specialized software such as REDUCE. The following simplifications, however, are very useful in order to avoid memory overflows. Using the relation

$$\gamma^\mu \Lambda_{\mu\nu} = \frac{1}{3m_*}(p^2 - m_*^2)\left[-\gamma^\nu + 2\frac{p^\nu}{m_*}\right], \tag{12}$$

one finds, for instance,

$$\begin{aligned}
\mathcal{A}_t = -g_s^2 \frac{\lambda^b \lambda^c}{4} \bar{u}_\mu \Bigg[&\frac{2}{3m_*^2} (\varepsilon_1^\mu \varepsilon_2^\nu \not{q} - \varepsilon_1^\mu \not{\varepsilon}_2 q^\nu - \varepsilon_2^\nu \not{\varepsilon}_1 q^\mu) \\
&+ \frac{1}{D_t} \not{\varepsilon}_1 \Lambda^{\mu\nu} \not{\varepsilon}_2 \Bigg] v_\nu \ .
\end{aligned} \tag{13}$$

This form may be also recovered directly on using a transformed Rarita-Schwinger field [see (4)] with $r = -\frac{1}{2}$.

Using all this, we find the cross section for gluon-gluon fusion into a pair of spin-$\frac{3}{2}$ quarks:

$$\sigma=\frac{\pi\alpha_s^2}{116640s}\left[60\ln\left[\frac{1+\beta}{1-\beta}\right](66y^2+35y+319+3726y^{-1}+1296y^{-2})+\beta(24y^4+1583y^3-20781y^2+32710y-108540-427680y^{-1})\right], \quad (14)$$

where $y=s/m_*^2$ and $\beta=\sqrt{1-4/y}$. The main point to notice about (14) is that the cross section grows like s^3 at large energies. This is to be contrasted with the similar cross section for a pair of spin-$\frac{1}{2}$ quarks,[5] which behaves like s^{-1}. When we integrate over the partons momentum fractions x, we get from (14) a much more important contribution from large x values compared to the spin-$\frac{1}{2}$ case. This is the main reason for the difference in the production rates.

As the pointlike approximation is expected to be valid if the fermions are not too heavy, let us first apply these results to the existing colliders, the CERN SPS and the Fermilab Tevatron [see Figs. 2(a) and 2(b)]. The lower limit quoted for the top mass at the SPS corresponds to a cross section $\sigma\simeq 0.7$ nb. Let us assume a similar sensitivity for detecting a spin-$\frac{3}{2}$ quark, we find then from Fig. 2(a) a lower mass $m_*\simeq 55$ GeV. At the Tevatron, if we again suppose that the luminosity and the detection efficiencies are similar, a negative result would give us a lower bound $m_*\simeq 110$ GeV.

In Fig. 2(c) we show the results corresponding to the parameters of the future SSC, that is proton-proton collisions with $\sqrt{s}=40$ TeV. The rates for producing a Q^* pair here, appear to be considerably larger than those of a Q pair. Unfortunately, it is very likely that our amplitudes will violate unitarity bounds for a large range of masses in this case. From the strong-coupling models quoted in the Introduction, we expect that important corrections in this respect should come from finite-size effects, which give rise to form factors. This will be considered in more detail in the next section.

Because of phase space (if m_*-m is large) it may actually be more favorable to produce mixed pairs: $Q^*\bar{Q}$ (or $\bar{Q}^*Q$), let us discuss this process now.

B. $Q^*\bar{Q}$, $Q\bar{Q}^*$ pairs

The calculation is much more tedious than before, one reason being that we have twice as may graphs now (see Fig. 3). Another difficulty is that the amplitudes turn out not to be transverse, contrary to the case of $Q\bar{Q}$ (as was first pointed out in Ref. 18) or even $Q^*\bar{Q}^*$ [as one may easily check using (11) and (12)]. This means that the summation over gluon helicities must be performed using an axial-gauge type of formula:

$$\sum_\lambda \varepsilon_\mu(\lambda)\varepsilon_\nu^*(\lambda)=-g_{\mu\nu}+\frac{k_\mu^1 k_\nu^2+k_\nu^1 k_\mu^2}{k^1\cdot k^2}\ . \quad (15)$$

The resulting expression for the cross section involves very lengthy polynomials in the two variables m and m_* and we cannot reproduce it here. (We would be happy, however, to send the computer program to the interested

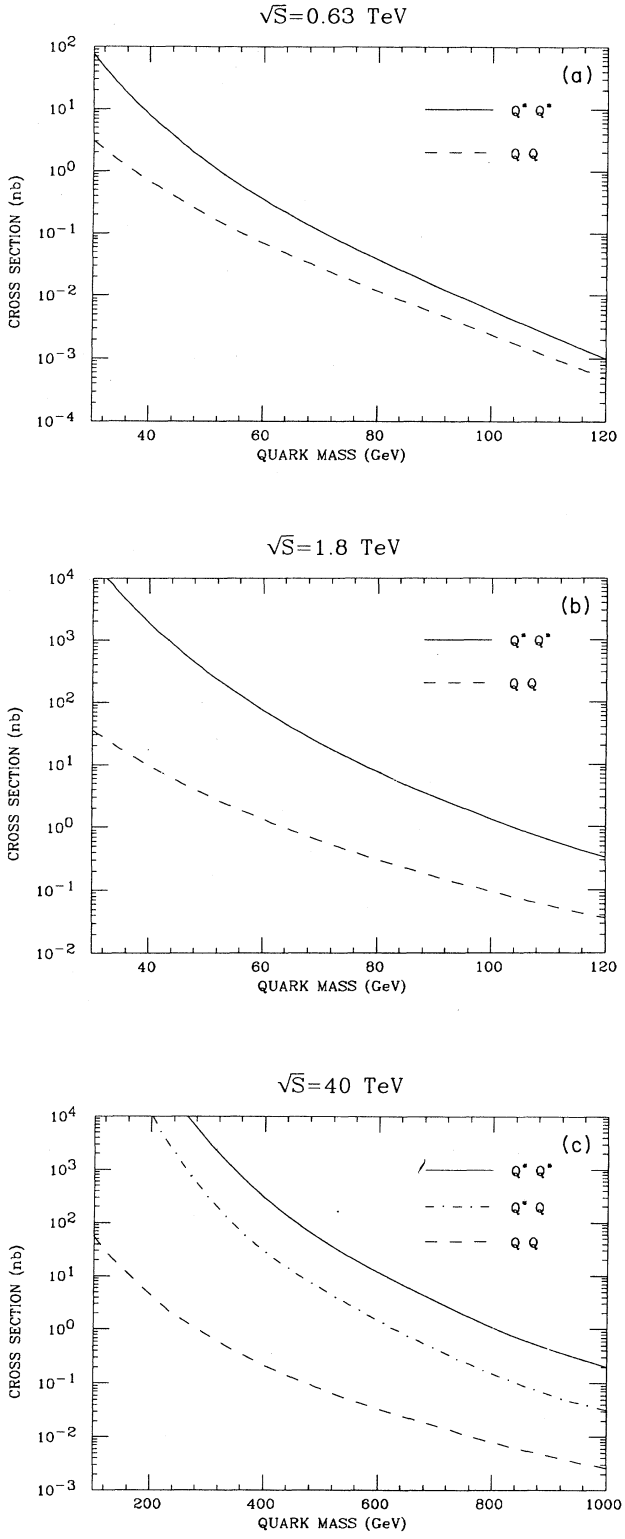

FIG. 2. Calculated total cross sections for the production of heavy-pointlike-fermion pairs in proton-antiproton collisions with $\sqrt{s}$: (a) 0.63 TeV, (b) 1.8 TeV, and (c) proton-proton collisions at 40 TeV. The solid line corresponds to $Q^*\bar{Q}^*$, the dotted-dashed one to $Q^*\bar{Q}$ and the dashed one to $Q\bar{Q}$. Equal masses are taken: $m_*=m$.

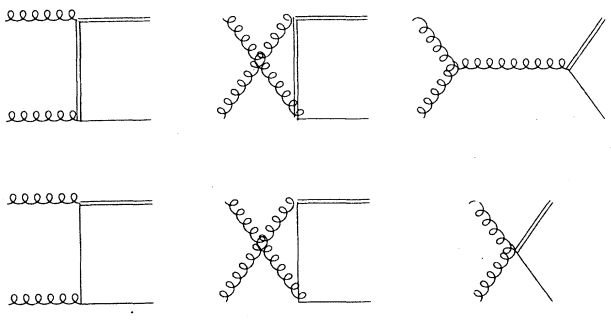

FIG. 3. Graphs which contribute to the production of a spin-$\frac{3}{2}$ plus spin-$\frac{1}{2}$ colored pair to lowest order in α_s.

reader.) Some numerical results can be appreciated from Figs. 2(c) and 4. In the latter, we have taken $m_*=2m$, we see that even then, it is still somewhat more favorable to produce the excited quarks in pairs. Let us now turn to the production of excited colorless fermion pairs.

C. $N^*\bar{N}^*$ and $N^*\bar{N}$

We use the notation N to designate the colorless fermions, as a reminder of the heavy nucleonic structures suggested in Ref. 8. Concerning production rates, our results would be practically the same as for leptons to the extent, however, that form-factor effects can be ignored, as we do here. The decay modes easily distinguish between the two possibilities. One may estimate, for instance, that the nuclear type N^* will emit a W and transform into an N, which will then emit several W's before decaying into a more stable baryon. The production mechanisms in the present case are those which are relevant for leptons (if we neglect interactions involving more than two partons). When the masses are lower than, say 100 GeV the Drell-Yan mechanism[19] dominates, that is, valence- or sea-quark–antiquark fusion into a photon or a weak boson. The situation changes at higher masses: for globally neutral pairs (N^+N^-) gluon-gluon fusion into γ, Z, or H via quark loops (see Fig. 5) may become much larger provided one assumes the existence of a heavy fourth generation of quarks. We shall do that here, and follow Ref. 3 by taking $m_Q=m_N$. We note that complete coherence would require us to consider including excited quarks as well into the loops. This will not be done here as it proves rather complicated technically, and necessitates the use of a cutoff. For the production of globally charged pairs (N^+N^0, for instance), the effectiveness of Z-W (described as a partons) fusion was recently demonstrated.[4] We will not consider this situation in this paper.

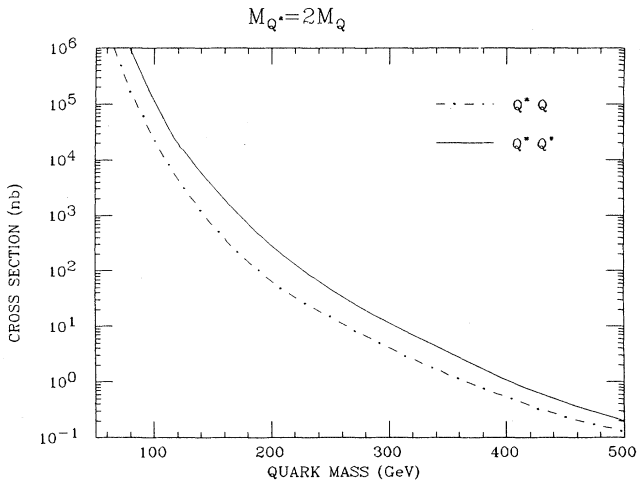

FIG. 4. Same as Fig. 2(c) except for the fermion masses: now $m_*=2m$.

Using (7) and (9), the result of the calculation of the two graphs in Fig. 5 is easily seen to differ from the spin-$\frac{1}{2}$-pair case by a simple proportionality factor:

$$\sigma_Z=\frac{\alpha^2\alpha_s^2 m_*^2\,|I(s)|^2\beta}{2048\pi\sin^4\theta_W\cos^4\theta_W m_W^4}\frac{4I_z^2}{9}(y-2y+10)\,,$$

$$\sigma_H=\frac{\alpha^2\alpha_s^2 m_*^2\,|J(s)|^2\beta^3}{512\pi\sin^4\theta_W m_W^4|1-z|^2}\frac{1}{9}(y^2-6y+18)\,, \qquad (16)$$

$$z=(m_H-i\Gamma_H/2)^2/s\,,$$

where

$$I(s)=\sum_Q 2I_z^Q Z\phi(Z),\quad J(s)=\sum_Q\frac{Z}{2}[1+(Z-1)\phi(Z)]\,,$$

$$\phi(Z)=\frac{1}{4}\left[\ln\frac{(1+\sqrt{1-Z})^2}{Z}+i\pi\right]^2,\quad Z=4m_Q^2/s\,,$$

and y has the same meaning as in (14). The two contributions were shown to add incoherently in Ref. 3, the argument goes through unmodified here too. Some numerical results are shown in Fig. 6, where we have taken for the quarks inside the loop $m_D=m_N$ and $m_U-m_D=150$ MeV (which is around the maximum value allowed by Veltman's ρ parameter[20] if one uses the value,[21] $\rho=1.006\pm0.008$). The curves correspond to $I_z=-\frac{3}{2}$, we see that the cross section for $N^*\bar{N}^*$ is again much larger than that for $N\bar{N}$.

The luminosity of the SSC is planned to be 2–3 orders of magnitude larger than those available at present. From this we may expect, broadly speaking, to be sensitive to phenomena occurring at the level of, say, 10^{-2} nb. This would allow the observation of our excited nucleons up to $m_N=6$–700 GeV. Unfortunately, their complicated decay patterns will make them rather difficult to recognize. Compared to the excited quarks, their production rates appear at first sight to be very small [com-

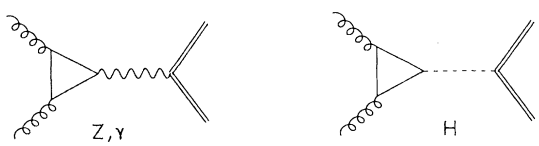

FIG. 5. Graphs which contribute to the production of a colorless spin-$\frac{3}{2}$ pair from gluon-gluon fusion. The Higgs-boson mass is set to 100 GeV.

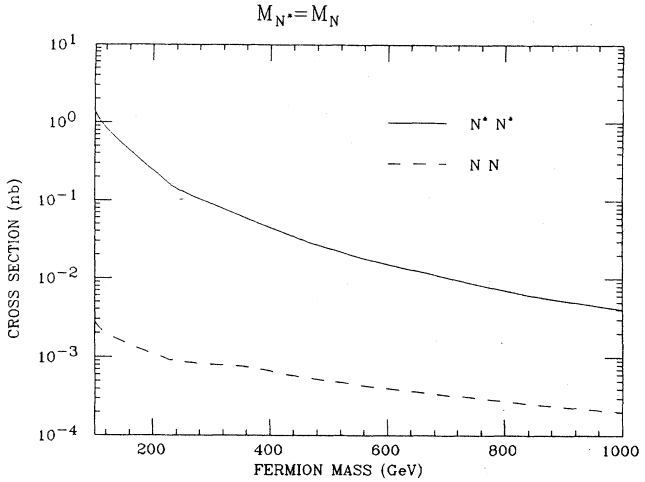

FIG. 6. Calculated cross sections for the production of a heavy colorless spin-$\frac{3}{2}$ pair (solid line) compared to the case of a spin-$\frac{1}{2}$ pair (dashed line), the masses being the same.

pare Figs. 2(c) and 4]. However, as we shall soon see, form-factor effects will strongly damp the former. Here, the form factor operates in a different kinematical region (the timelike one), where it is more difficult to anticipate its influence. It could well enhance the cross sections, for instance, it there is a close by resonance with the quantum numbers of the Z or the H.

IV. FORM FACTORS

In this section we mainly discuss the case of $Q^*\bar{Q}^*$. When the fermions cannot be considered as pointlike, the interaction vertices are no longer local and, as a consequence, they involve a function of the off-shell momentum. The first task is to estimate the cutoff occurring in this function. In low-energy hadronic physics, the best well-known form factors are the electromagnetic ones. There, a rather well-verified rule (the vector-meson-dominance principle[22]) states that the cutoff is provided by the masses of the lightest mesons with the same quantum numbers as the photon: ρ and ω. In our case, when Q^* is off shell, we are willing to boldly generalize this concept by estimating that the cutoff Λ is given by the mass of the next excitation with the same quantum numbers. An explicit model with a similar prediction is given in Ref. 23. Obviously, we do not know the mass of this Q^{**}, but we can estimate its value to be, perhaps, between $1.5m_*$ to a few times m_*. The precise functional dependence on q^* at one vertex is also unknown, we shall be using simple forms such as

$$\left[\frac{m_*^2-\Lambda^2}{q^2-\Lambda^2}\right]^n \tag{17}$$

and let n vary between $\frac{1}{2}$ and 2. We also make another assumption. In the absence of cutoff, diagram (c) in Fig. 1, although necessary to ensure gauge invariance, actually makes a very tiny contribution to the cross section, so one may neglect it and concentrate on the first two which involve virtual Q^* exchange. One cannot tell whether this remains correct when form factors come into play since they precisely diminish the contribution of these diagrams. The third one will also be affected but the cutoff could be different (in fact, if there is anything like an excited gluon, it may well become dominant). Loss of gauge invariance may be worrisome but the order of magnitude of the result is not likely to be modified by gauge transformations.

Bearing all these uncertainties in mind, the influence of the form factors can be appreciated from Fig. 7(a) and 7(b). When Λ is very large, we check that we recover very closely our preceding results (the two curves are nearly undistinguishable). Note that technically, the angular integration is performed numerically now. The effect can be rather mild if n is small and Λ large enough, like $n=\frac{1}{2}$ and $\Lambda=5m_*$. A more realistic choice perhaps is $n=1$, $\Lambda=2m_*$ which leads to a more severe reduction of the cross sections by a factor 10 to 100. Various possi-

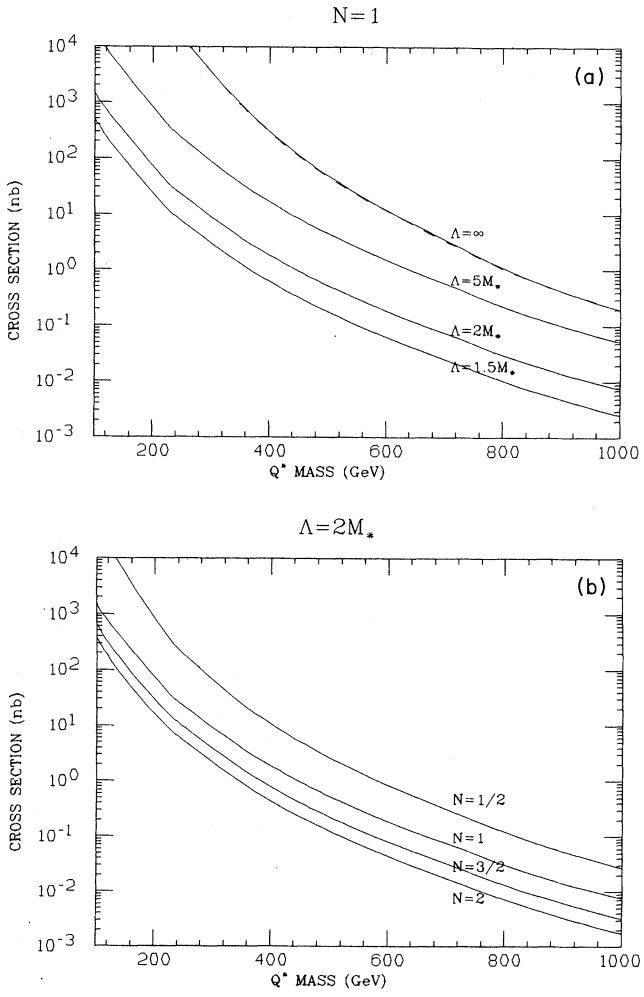

FIG. 7. $Q^*\bar{Q}^*$ production cross section in the presence of a vertex form factor [see (17) in the text]: (a) n is fixed to one and Λ is varied, the dashed curve corresponds to the complete pointlike calculation. (b) Λ is fixed to $2m_*$ and n is varied.

bilities are represented in Fig. 7. If Λ is very close to m_* the numerator in (17) becomes very small. These forms cannot be trusted in such a case. The exponent, n has a double role, it decreases the overall value of the form factor and smoothes the large-s behavior of the elementary cross section, thereby rendering the x integration in (10) less effective. If we use again our estimate that the lowest observable cross section is between 10^{-3} and 10^{-2} nb at the SSC, we see from Fig. 7 that it is likely that one will be able to observe spin-$\frac{3}{2}$ quarks up to $m_* \simeq 1$ TeV.

V. DECAY PROPERTIES

For detectional reasons it is obviously important to try to figure out what are the main decay modes of our excited fermions. If their total width turns out to be too large, these states will be quite elusive. Based on their model, Schechter and Johnson find that the main decay channel is

$$Q^* \to W_L(Z_L) + Q \ ,$$

where the subscript L indicates that longitudinal-polarization states are involved. In this section, we examine the consequences of assuming that the excited quarks can be classified in the standard model according to weak isospin. If we return to our assumption of point-like particles then we may still have pure $V-A$ coupling to the gauge bosons, which allows us to classify the left-handed fermions into the isospin-$\frac{3}{2}$ representation and the right-handed ones into isospin 0. The part of the Lagrangian which does not contain Φ was written in (8), we see immediately a qualitative difference with Ref. 8: longitudinal-polarization states cannot be singled out by this interaction. When the energy of the weak boson is much larger than its mass, for instance, we have $\varepsilon_\mu(0) \sim p_\mu / m_W$, and the combinations like $\partial_\mu W_\nu - \partial_\nu W_\mu$ which occur in (8) vanish to leading order. Let us now show that this result is unchanged if we take interactions including Higgs fields. The only invariant forms [according to gauged SU(2)×U(1)] containing one or two Higgs fields are of the following type:

$$\begin{aligned} &\bar{L} R^d_\mu D^\mu \Phi, \quad \bar{L} R^u_\mu D^\mu \bar{\Phi} \ , \\ &\bar{R} \gamma_\nu R^i_\mu D^\nu \Phi^\dagger D^\mu \Phi, \quad \bar{L} \bar{T}^\dagger \gamma_\nu L^i_\mu D^\nu \Phi^\dagger \tau D^\mu \Phi \end{aligned} \tag{18}$$

(and Hermitian conjugates) where $L = (U_L D_L)^T$, similarly L_μ is constructed out of the multiplet left-handed Q^*'s, and we have noted

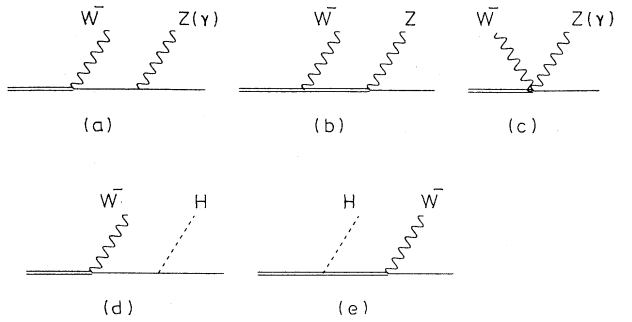

FIG. 8. Lowest-order graphs for three-body decays of $Q^*(I_z = -\frac{3}{2})$: (a)–(c) lead to W, Z (or γ), and D, while (d),(e) lead to W, H, and D.

$$R^{u(d)}_\mu = \tfrac{1}{2}(1+\gamma_5) Q^*[I_z = \tfrac{1}{2}\ (-\tfrac{1}{2})] \ .$$

In the unitary gauge, we see that the first two forms will lead to direct coupling to the gauge fields, but observe that two isospin components of Q^* only ($I_z = \pm\frac{1}{2}$) are involved. The other two components occur in the last two interactions in (18), but these lead to decays with a higher multiplicity, with two gauge bosons, or one Higgs and one gauge boson and so on.

The multiplet member with lowest isospin, $Q^*(I_z = -\frac{3}{2})$, is the most promising one. On the one hand, it is expected to have the smallest mass (at least if we naively extrapolate from the known fermion doublets) which makes it the easiest one to produce. Furthermore, it is not subject to intramultiplet cascading which will be very rapid for the other multiplet members if the mass splittings are larger than m_W. Finally, from what we have argued above, its decays into unexcited fermions may be inhibited to some extent. We note also that the two decay modes $Q^*_{(-3/2)} \to \gamma Q$ and $Q^*_{(-3/2)} \to HQ$ are forbidden.

Another consequence of this discussion is that decays involving two gauge bosons, which are of higher order in α, may become unexpectedly important if the mass difference $m_* - m$ is large enough. This is because longitudinal polarizations are not suppressed in this case, and we saw that their module grows with the energy (contrary to the transverse-polarization states). Let us now make some estimates on all this.

We start from the state Q^* $(I_z = -\frac{3}{2})$, the only single boson decay mode is

$$Q^* \to W^- + D \ .$$

Using (8) it is a relatively easy matter to find the rate:

$$\Gamma = \frac{\alpha\kappa^2}{24 \sin^2\theta_W \cos^2\theta_W} \frac{3m_*^6 - m_*^4(5m^2 - m_W^2) + m_*^2(m^4 - m_W^4) + (m^2 - m_W^2)^3}{m_*^4 (m_* + m)^2} Q_{\text{c.m.}} \ , \tag{19}$$

where $Q_{\text{c.m.}}$ is the c.m.-system momentum.

We consider now three-body decay modes. The three graphs contributing to $Q^* \to W^- Z D$ are represented in Figs. 8(a)–8(c). Other modes with two weak bosons will involve the U quark and should be smaller because of phase space and furthermore the U quark is unstable. We shall present an approximate evaluation of the amplitude based on the following remark. In the first two

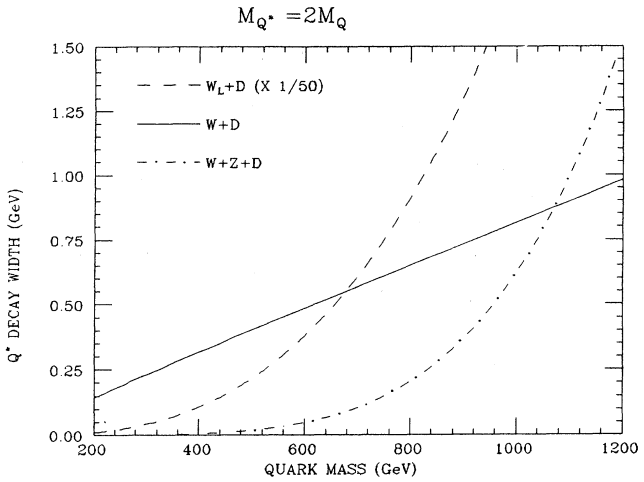

FIG. 9. Calculated decay widths of Q^* under the assumptions of Sec. IV. The solid line is for the two-body decay mode $Z+D$ and the dashed-dotted line for the three-body mode $W+Z+D$. For comparison, the dashed line represents the decay into a longitudinal W and D.

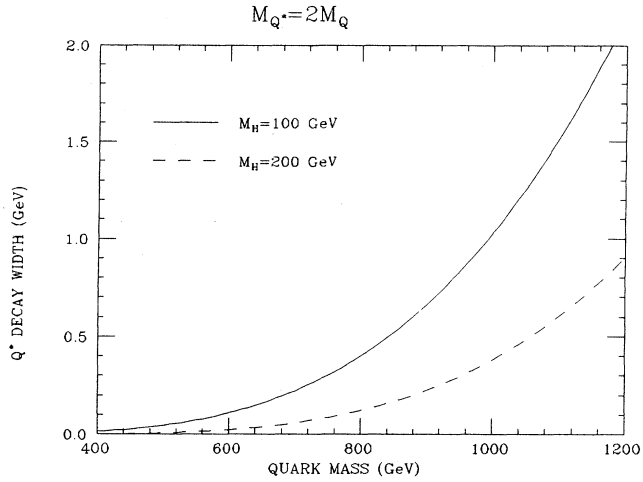

FIG. 10. Decay width involving a Higgs boson for two values of the Higgs-boson mass as a function of the excited quark mass.

graphs, one of the longitudinal polarizations is suppressed (at the Q^*Q vertex), while they are both unsuppressed in the third graph. This one is therefore expected to dominate when large momenta become involved. As we mentioned before, it is precisely in this situation that we expect this higher-order decay mode to matter. We content ourselves with calculating this last graph. Numerical results are presented in Fig. 9 in which we choose $m_*=2m$ and κ [see (8)] equal to 1. We see that the simple decay mode dominates in a fairly large range: up to $m_*\simeq 2$ TeV at higher masses three-body modes grow very rapidly. Provided κ does not take unreasonably large values, it appears that the total width of this Q^* will remain smaller than $\simeq 1$ GeV, which is a surprisingly small value for such high-mass hadrons. For comparison, we have also plotted the width corresponding to a decay involving a longitudinal W, using (with some extrapolation) an axial-vector form factor from Refs. 8 and 9. Finally, we have evaluated the rates for producing a Higgs boson. There are two relevant graphs shown in Figs. 8(d) and 8(e) and some results are represented in Fig. 10. If the Higgs-boson mass is rather small, e.g, 100 GeV, then the rate is quite similar to that for two gauge bosons, which is quite small, as we saw, unless m_* is larger than 2 TeV.

VI. CONCLUSION

Inspired by the model of Johnson and Schechter we have discussed some production and decay properties of spin-$\frac{3}{2}$ fermions. Two distinct scenarios were considered which lead to rather different conclusions.

(a) If one strictly respects the Johnson-Schechter model (except for the values of the masses) then the fermions are extended objects, and their production has to be discussed in connection with form factors. It is difficult to make precise predictions but it is clear from Sec. IV that unimpressive rates are normally expected. The benefit of having a spin-$\frac{3}{2}$ exchange in some of the diagrams is washed out to a large extent by the form factors. In this picture, ordinary quarks too have an extended structure which are likely to deplete their cross sections as well.

(b) If one simply assumes the existence of heavy quarks and heavy excited quarks, yet that they are sufficiently pointlike to be ascribed definite representations in the standard model, their properties are more spectacular. The production rates were seen in Sec. III to be quite large, and the total width is surprisingly narrow, with two-particle decay modes dominating. Only experiment, of course, can decide if any of these pictures makes sense.

ACKNOWLEDGMENTS

Division de Physique Théorique is Laboratoire associé au CNRS.

[1]UA1 Collaboration, C. Albajar *et al.*, Z. Phys. C **37**, 505 (1988).
[2]E. Eichten, I. Hinchliffe, K. Lane, and C. Quigg, Rev. Mod. Phys. **56**, 579 (1984).
[3]S. S. C. Willenbrock and D. A. Dicus, Phys. Lett. **156B**, 429 (1985).
[4]S. Dawson and S. S. C. Willenbrock, Nucl. Phys. **B284**, 449 (1987).
[5]B. L. Combridge, Nucl. Phys. **B151**, 429 (1979).
[6]P. Nason, S. Dawson, and R. K. Ellis, Nucl. Phys. **B303**, 607 (1988); C. Altarelli, M. Diemoz, G. Martinelli, and P. Nason, *ibid.* **B308**, 724 (1988).
[7]V. Barger *et al.*, Phys. Rev. D **35**, 3366 (1987).
[8]R. Johnson and J. Schechter, Phys. Rev. D **36**, 1484 (1987).
[9]V. Soni, B. Moussallam, and S. Hadjithedoridis, Phys. Rev. D **39**, 915 (1989).
[10]G. S. Adkins, C. R. Nappi, and E. Witten, Nucl. Phys. **B228**, 552 (1983; S. Kahana, G. Ripka, and V. Soni, Nucl. Phys. **A415**, 351 (1984); M. C. Birse and M. K. Banerjee, Phys. Lett.

136B, 284 (1984).
[11]M. S. Chanowitz, M. A. Furman, and I. Hinchliffe, Nucl. Phys. **B153**, 402 (1979).
[12]R. Johnson and J. Schechter, Syracuse report, 1988 (unpublished).
[13]G. F. Chew and F. E. Low, Phys. Rev. **101**, 1570 (1956).
[14]W. Rarita and J. Schwinger, Phys. Rev. **60**, 61 (1941).
[15]P. van Nieuwenhuizen, Phys. Rep. **68**, 189 (1980).
[16]H. T. Williams, Phys. Rev. C **31**, 2297 (1985).
[17]R. D. Peccei, Phys. Rev. **181**, 1902 (1969).
[18]H. Georgi, S. Glashow, M. Machacek, and D. Nanopoulos, Ann. Phys. (N.Y.) **114**, 273 (1978).
[19]S. D. Drell and T. M. Yan, Ann. Phys. (N.Y.) **66**, 578 (1971).
[20]M. Veltman, Nucl. Phys. **B123**, 89 (1977); A. Cohen, H. Georgi, and B. Grinstein, *ibid.* **B232**, 61 (1984).
[21]Particle Data Group, M. Aguilar-Benitez *et al.*, Phys. Lett. **170B**, 78 (1986).
[22]M. Gell-Mann and F. Zachariasen, Phys. Rev. **124**, 953 (1961); J. J. Sakurai, Phys. Rev. Lett. **8**, 79 (1962).
[23]R. Bryan, C. Dominguez, and B. VerWest, Phys. Rev. C **22**, 160 (1980).